Curing effects on fracture of High-Performance Cement Based Composites with Hybrid Steel Fibers

F. Ozalp, Y. Akkaya, C. Sengul, B. Akcay, & M.A. Tasdemir
Istanbul Technical University, Civil Engineering Faculty, Istanbul, Turkey

A.N. Kocaturk
Iston, Prefabricated Concrete Products and RMC Co., Istanbul, Turkey

ABSTRACT: In this work, effects of fiber strength and curing conditions on the mechanical behaviour and fracture properties of high performance cement based composites with hybrid steel fibers were investigated. Depending on the high temperature curing conditions, concretes with hybrid steel fibers showed behaviour of enhanced toughness and ductility. Fracture energy of the matrix increased up to 96 times owing to normal strength steel fibers, while in concretes with high strength steel fibers the increase in fracture energy due to steel fibers was 168 times. Petrographic examinations indicated that a connected crack system occurred which was filled with calcium hydroxide at 200°C curing condition and no indication of delayed ettringite formation was observed. Furthermore, the prefabricated elements successfully produced with these materials, such as gully tops and manhole covers used in the city infrastructure, are presented along with selected examples from several applications.

1 INTRODUCTION

There have been incredible advances in concrete technology over the years. Not more than 45 years ago the maximum compressive strength obtained at the construction site was about 40 MPa, such a concrete is now considered quite low strength when compared to the modern very-high strength concretes with cube compressive strengths between 200 MPa and 800 MPa, tensile strengths between 25 MPa and 150 MPa, and fracture energies of about 30000J/m^2 (Alexander 1993, Richard & Cheyrezy 1995, Dugat et al. 1996, Bonneau et al. 1997). In recent years, a number of specific developments have occurred in parallel to the evolution of what is commonly described as high performance concretes. Such concretes have high strength combined with highly enhanced durability. The brittleness of concrete, however, increases with an increase in its strength. In other words, the higher the strength of concrete, the lower is its ductility. This inverse relation between strength and ductility is a serious drawback and limits the use of high strength concrete (Balaguru et al. 1992). Their potential use is yet to be established and more work is required, in particular, to evaluate their long-term performance. These materials have already successfully been laboratory tested for strengthening structures and their potential use in areas subjected to earthquakes needs to be further investigated (Ilki et al. 2004).

The fracture energies of Reactive Powder Concretes (RPCs), thus, are about 300 times that of normal strength concrete or even 1350 times for Slurry Infiltrated Fiber Reinforced Concrete (SIFCON) (Fritz 1991). The low porosity of RPC gives it important durability and low transport properties and makes it potentially suitable for some structures exposed to harsh environmental conditions (Feylessoufi et al. 1996, Matte & Moranville 1999).

The interface between cement paste and aggregate particles is the weakest zone in concrete, and the use of ultra-fine particles, such as silica fume, is important for densification and for the improvement of the stability of fresh concrete, thus, enhancing the overall durability and strength. Micro-silica or silica fume is a by product of silicon and ferrosilicon industries; it has been used since 1950s to improve the properties of concrete. To gain benefits from these particles, good dispersion within the concrete system is necessary and can be provided by means of a superplasticizer (Tasdemir et al. 1998, Tasdemir et al. 1999). The internal structure of RPC is optimized by precise gradation of all particles in the mixture, to add short steel fibers for improved ductility and to allow the resulting concrete to harden under pressure and increased temperatures (Walraven 1999).

The main objective of the work presented here is to demonstrate the combined effects of curing conditions, and the hybrid steel fibers and their strengths on the mechanical and fracture properties of high performance steel fiber reinforced composites.

2 EXPERIMENTAL WORK

2.1 *Materials and mix proportions*

A total of 6 composite mixtures were cast for this investigation. In all the mixtures, the volume fractions of cement, siliceous sands (0-2 mm and 0-0.5 mm), silica fume and water were kept constant. Cement used was ordinary Portland cement with a density of 3.20 g/cm³ and its nominal content in the composite was 1000 kg/m³. The maximum particle size of aggregate was 2 mm and the density of siliceous sand was 2.65 g/cm³. The amount of high-range water reducing admixture (HRWRA) varied between 11 % and 12 % by weight of cement for different composite mixtures to maintain the same workability. Three different steel fibers with and without hooked ends were added. The short ones without hooked ends were straight high strength steel fibers coated with brass, 6 mm in length, 0.16 mm in diameter and the aspect ratio (L/d) was 40. The tensile strength of normal and high strength hooked end steel fibers were 1150 and 2250 MPa, respectively, while their aspect ratios were the same (l/d=55). The total volume fractions of fibers were kept constant at 3%. The mixture proportions of the matrix were as follows; cement: silica fume: water: siliceous sand (0.5-2 mm): siliceous powder (0-0.5 mm): HRWRA = 1: 0.250: 0.114: 0.325: 0.493: 0.120. Partial replacement of aggregate by steel fiber was based on one to one volume basis. The properties of the steel fibers are given in Table 1.

Table 1. The properties of straight and hooked-end steel fibers

	Type of steel fiber		
	High strength straight steel fiber (HSSSF)	Normal strength hooked-end steel fiber (NSHSF)	High strength hooked-end steel fiber (HSHSF)
Length (L) mm	6	30	30
Diameter (d) mm	0.15	0.55	0.55
Aspect ratio (L/d)	40	55	55
Tensile strength (N/mm²)	2200	1100	2200

The composite mixtures were designated using the following codes: P=matrix, R=composite with high strength straight steel fibers, S=composite with normal strength hooked-end steel fibers, T=composite with high strength hooked-end steel fibers. RS and RT contain equal percentages of steel fibers; 1.5%HSSSF+1.5%NSHSF and 1.5%HSSSF+ 1.5%HSHSF as shown in Table 2.

Table 2. The designation of the mixtures

Mix Code			Steel fiber percentage		
Normal curing	Steam curing at 65°C	Hot curing at 200°C	HSSSF	NSHSF	HSHSF
PN	PV	PZ	0	0	0
RN	RV	RZ	3	0	0
SN	SV	SZ	0	3	0
TN	TV	TZ	0	0	3
RSN	RSV	RSZ	1.5	1.5	0
RTN	RTV	RTZ	1.5	0	1.5

2.2 *Specimen preparation*

In all mixtures, because the efficiency of HRWRA was low, over dosage was required. For reaching the high values of strength, cement and silica fume content were significantly increased, thus the water/binder ratio decreased. Because of the fact that 60% of the HRWRA is composed of water, water/cement and water/binder ratios were recalculated and expressed with the names of the total water/cement and total water/binder ratios. Hence, the total water/binder ratio in the mixtures was 0.17.

In mixing, cement, silica fume, siliceous sand, and siliceous powder were blended first in dry condition. Halves of the HRWRA and the water were mixed in a pan and added to the mixture. The remaining halves of the HRWRA and the water were added to the mixture gradually to provide homogeneity in the mixture. Steel fibers were scattered in the mixture and carefully mixed to achieve a uniform distribution. The specimens were cast in steel moulds and compacted on a vibration table. Details of the tests and dimensions of the specimens are given in Table 3.

Table 3. Test methods and specimen size

Test type	Specimen	Dimensions (mm)	Parameters
Compression	cylinder	Ø100, h200	f'_c (MPa), E (GPa)
Splitting	disc	Ø150, h60	f_{st} (MPa)
Bending	beam	70×70×280	G_F(N/m), f_{flex} (MPa)

f'_c =compressive strength, E= modulus of elasticity, f_{st}=splitting tensile strength, G_F =fracture energy, f_{flex} =flexural strength.

All specimens were demoulded after 24 hours, and then three different curing regimes were applied: i) Steam curing was as follows; an initial moisture curing for one day was followed by steam curing of 65°C at atmospheric pressure for 3 days and further in a water tank saturated with lime at 20°C until testing day. ii) The period of hot curing regime was similar to the steam curing regime; however, a higher temperature of 200°C was applied to the specimens. During this high temperature curing regime, specimens were wrapped by the two layered

wrapping material. The first layer wrapping material was a high temperature resistant plastic sheet and the second one was an aluminium foil. iii)The third curing regime involved standard water curing in a water tank saturated with lime at 20°C prior to testing.

2.3 *Test procedure*

The tests for determining the fracture energy (G_F) were performed in accordance with the recommendation of RILEM 50-FMC Technical Committee. As schematically shown in Figure 1, the deflection was measured using a linear variable displacement transducer (LVDT). The load was applied using a closed-loop testing machine (Instron 5500R) with a maximum capacity of 100 kN. The beams prepared for the fracture energy tests were 280 mm in length and 70 mm × 70 mm in cross section. The notch to depth ratios (a/D) of specimens were 0.40 and the notches were formed using a diamond saw. The effective cross section was reduced to 70 mm × 42 mm to accommodate long fibers in more abundance, and the length of support span was 200 mm. The crack mouth opening displacement (CMOD) was used as a feedback control variable to obtain stable tests. Thus, load versus CMOD and load versus displacement at the midspan (δ) curves were obtained for each specimen.

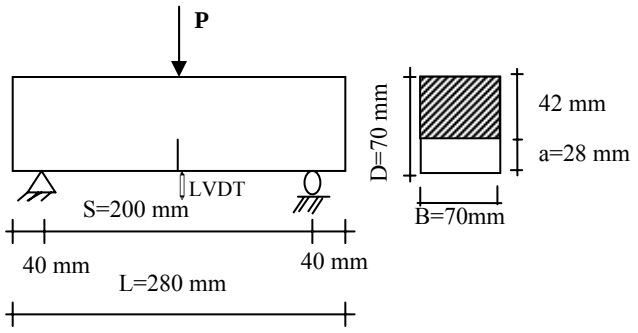

Figure 1. Schematic representation of the three point bending test.

The fracture energy was determined using the following expression

$$G_F = \frac{W_0 + mg\dfrac{S}{U}\delta_s}{B(D-a)} \qquad (1)$$

where, B, D, a, S, U, m, δ_s, and g are the width, depth, notch depth, span, length, mass, specified deflection of the beam and gravitational acceleration, respectively. At least five specimens of each mixture were tested at the 56th day. All the beams were loaded at a constant rate of 0.02 mm/minute. The fracture energy of the matrix is based on the area under the complete load versus displacement at mid span curve. The results for composites with steel fibers are based on the area under the load versus displacement curve up to a specified displacement. A cut-off point was chosen at 10 mm displacement. It is seen from Figure 2 that the energy at this displacement (i.e. 10 mm), however, is not totally dissipated.

In order to determine the ductility of the composites, characteristic length (l_{ch}) was calculated using the measured G_F, E, and f'_t, according to the Eq(2) introduced in fictitious crack model by Hillerborg et al. (1976).

$$l_{ch} = \frac{EG_F}{f_t'^2} \qquad (2)$$

where f'_t, E, and G_F are direct tensile strength, modulus of elasticity, and fracture energy, respectively.

In this study, the term "direct tensile strength (f'_t)" in this relation was replaced by "splitting tensile strength (f_{st})".

3 EXPERIMENTAL RESULTS AND DISCUSSION

Table 4 summarizes the mechanical test results of composites produced and their fracture parameters.

3.1 *Compressive strength and modulus of elasticity*

A significant increase is observed in compressive strength of composites with increasing curing temperature. The composites containing high strength straight fibers have the highest compressive strength for all curing conditions. In addition, compressive strengths of composites with high strength hooked-end steel fibers are higher than those with normal strength hooked-end steel fibers. As seen in Table 4, it is clear that high temperatures activate the pozzolanic reaction between the calcium hydroxide formed during the normal cement hydration and silica fume contained in the mixture. On the other hand, the reaction may take place between the very fine ground silicious sand and calcium hydroxide product at hot curing conditions (Alaee 2002, Massaza & Costa 1986). It is also clearly shown that the high temperature curing conditions may provide a shorter curing period compared to the standard curing regime.

There is no significant effect of the type of steel fibers and their strengths, and curing conditions on the modulus of elasticity. In composites with hooked-end fibers, however, the fiber strength causes little increase in the modulus of elasticity.

Table 4. Fracture and strength properties of composites

	Mix code	f'_c (MPa)	E (GPa)	f_{st} (MPa)	G_F (N/m)	f_{flex} (MPa)	l_{ch} (mm)
Normal curing	PN	131.2	44.1	8.7	181	10.2	105
	RN	146.7	45.4	12.4	6043	23.8	1784
	SN	113.4	41.6	13.5	14254	35.2	3254
	TN	130.0	45.9	15.6	21617	37.7	4077
	RSN	143.7	44.6	15.0	8067	28.1	1599
	RTN	133.1	48.1	15.1	19829	38.5	4183
Steam curing at 65°C	PV	136.3	44.1	9.4	201	12.8	100
	RV	175.1	45.1	15.5	6778	25.4	1272
	SV	133.8	38.5	16.0	14079	37.4	2117
	TV	149.8	45.1	17.0	24821	44.9	3873
	RSV	144.3	42.8	15.4	10343	35.7	1867
	RTV	149.4	41.3	17.6	20140	45.8	2685
Hot curing at 200°	PZ	145.2	41.5	6.2	179	8.6	193
	RZ	177.0	45.6	16.0	5421	23.2	966
	SZ	136.0	38.8	16.4	17212	41.1	2483
	TZ	156.4	41.3	16.7	30169	42.0	4468
	RSZ	163.4	34.8	16.9	11336	36.6	1381
	RTZ	168.2	43.9	17.3	20235	46.8	2968

3.2 *Splitting tensile and flexural strengths*

As seen in Table 4, the splitting tensile and flexural strengths of composites notably increased with addition of fibers as expected. In addition, composites containing longer fibers (S and T) have significantly greater splitting tensile strength than those containing short fibers (R), while the increasing tensile strength of steel fibers increased the splitting tensile strength of composites.

The use of hybrid fibers enhanced the splitting tensile strength of the composites. Depending on the type and strength of the fibers, and curing conditions, splitting and flexural strengths increased up to 5 times compared to those of the matrix. It is also indicated in Table 4 that the curing temperature increased the splitting and flexural strengths of composites. Since hot curing regimes activate pozzolanic reaction and enhance the microstructure of the composites, both splitting and flexural strengths can be greatly improved. On the other hand, the hot curing condition significantly reduced these strengths of plain composite. This is due to the fact that higher curing condition caused the formation of the microcracks in the matrix phase and this in turn, caused reduction in the splitting tensile strength. In addition, the composites containing both straight and high strength hooked-end steel fibers (RT) have the highest splitting and flexural strengths. Along the fracture plane of the composites in both splitting and bending tests, the opening and propagation of the crack are controlled by the steel fibers. During crack propagation some fibers are broken, but some are pulled-out of the matrix. After completion of the splitting and bending tests, the fracture surfaces were examined. In most cases the high strength hooked-end fibers did not break, but were pulled-out of the matrix.

In some other cases the normal strength hooked-end fibers were broken into two parts. Thus, in the latter case, the mechanical mismatch may have played a role on these two mechanical properties. As indicated earlier, high strength steel fiber with a tensile strength of 2000 MPa is suggested for the high strength concretes (Vandewalle 1996, Grünewald & Walraven 2002).

3.3 *Fracture energy*

The test results have shown that the most significant effects of both fiber addition and curing condition are observed on the fracture energy of composites. Figures 2 and 3 show the effects of curing conditions, and the type and strength of the steel fibers on the mechanical behaviour of the composites. In Figure 2, each composite shows the brittle behaviour of a typical matrix. It is seen that the use of high strength steel fibers improves the mechanical performance and increases the fracture energy of the composite. Especially after the first crack, the formation of strain hardening in the ascending branch of the curve is a typical indication of high performance cementitious composites. The composites with normal strength hooked-end steel fibers have lower peak loads and steeper gradients of the softening branch compared to the composites with high strength hooked-end steel fibers and the highest fracture energies were obtained from these composites.

As seen in Table 4, curing regimes enhance the microstructure of the composites and as a result the fracture energy has been greatly improved. It can be concluded that increasing the curing temperature increased the peak load significantly and this resulted in an increase in fracture energy, while the slope of the ascending branch of the curves remained almost constant.

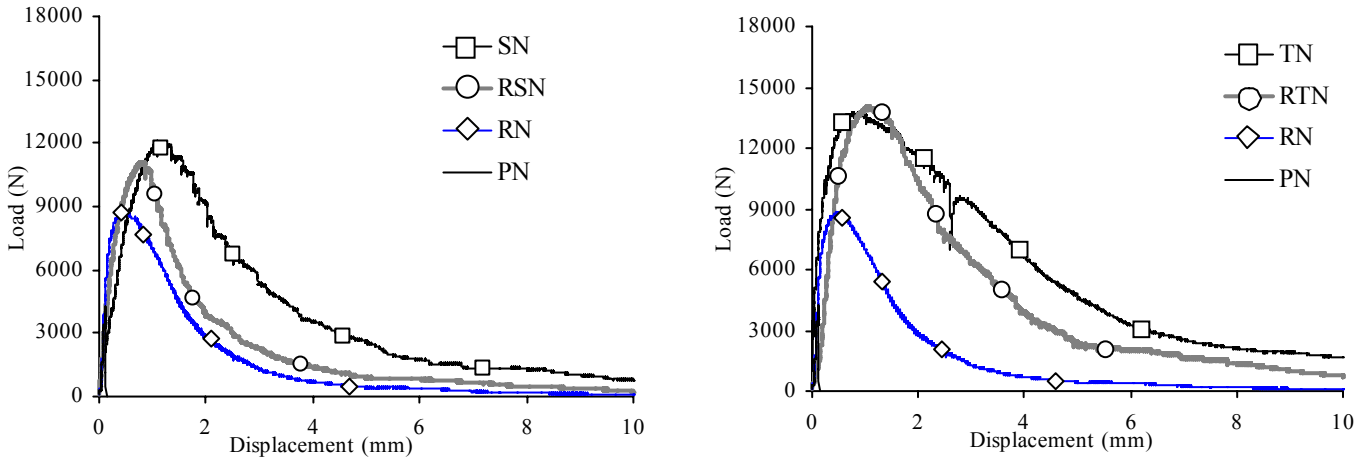

a) normal curing (N)

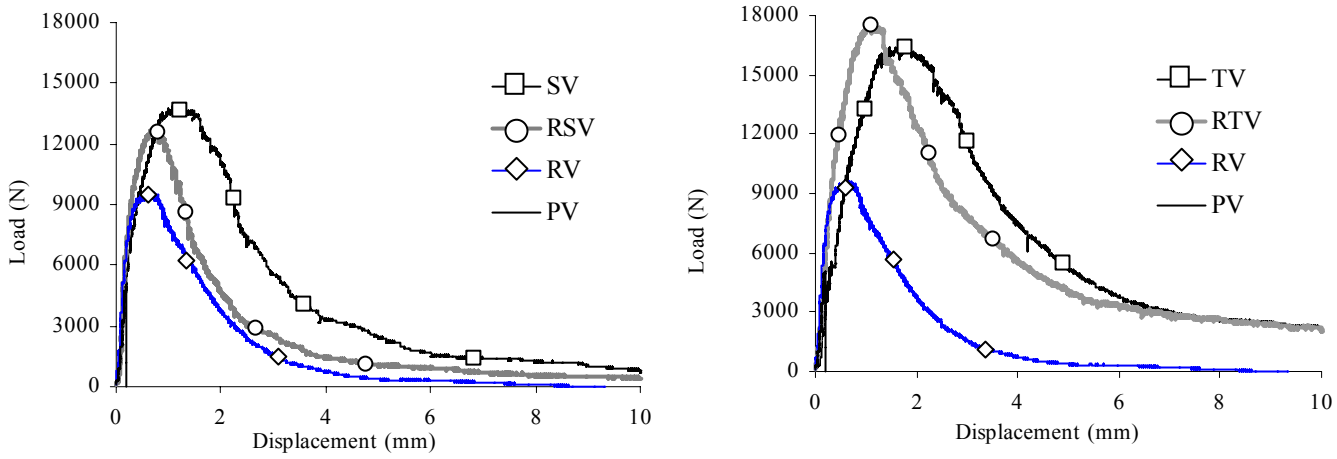

b) steam curing (V)

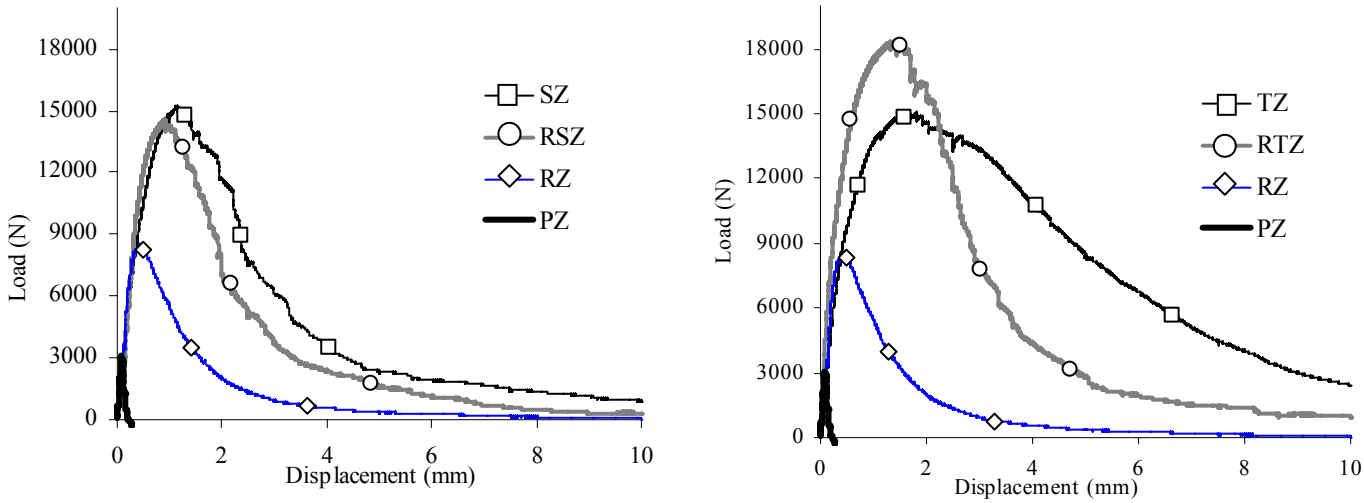

c)hot curing (Z)

Figure 2. Typical load versus displacement curves for composites at different curing regimes: a) Normal curing, b) Steam curing c) Hot curing.

The increase in the fiber aspect ratio and also the fiber tensile strength significantly increased the fracture energy of composites. The short fibers have a limited effect on the post-peak response of load versus displacement at midspan of beam, while there is a substantial effect of long fibers on the post peak response part of curve, which results in high value of fracture energy.

It is also shown that, depending on the high temperature curing condition, fracture energy of the matrix increased up to 168 times compared to composites with high strength steel fibers; while in composites with normal strength steel fibers the increase in fracture energy due to the steel fibers was 96 times.

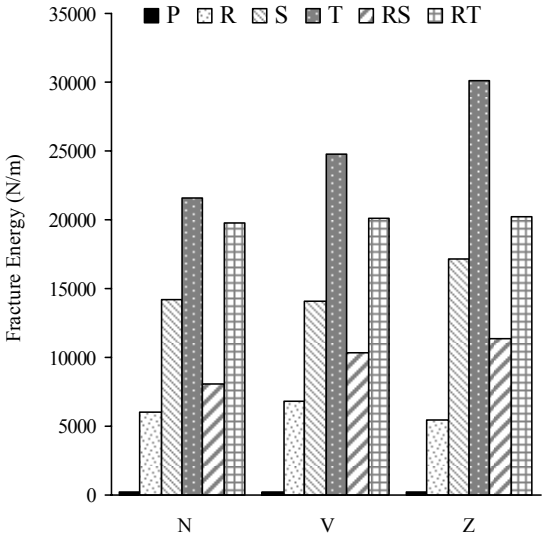

Figure 3. The variation of fracture energy with curing condition and type of steel fibers.

In all curing regimes, while the composite hybrid mixture of high strength straight and high strength hooked-end steel fibers (i.e. mixture RT) have the highest peak load, the fracture energy of composites with high strength hooked-end steel fibers (i.e. mixture T) have been found greater than those of other series.

3.4 *Characteristic length*

Characteristic length (l_{ch}) should be taken into consideration in the design of cementitious composites, because it controls the nominal strength, failure mode, and crack pattern (Lange-Kornbak & Karihaloo, 1998). The variation of l_{ch} with curing conditions, and the types and the strengths of steel fibers are shown in Table 4. As curing temperature, the aspect ratio and strengths of fibers increase, the characteristic length, which is a measure of ductility of the material, increases significantly.

4 PETROGRAPHIC EXAMINATION

In order to investigate the effects of high temperature curing on the microstructure, polished plane and thin sections of samples were prepared. For the plane sections, composite samples with a cross-sectional area of 10 × 7.5 cm were cut and impregnated with fluorescence epoxy under vacuum. The fluorescence in the epoxy enters the microcracks and macrocracks, capillary, entrained and entrapped air voids, starting from the surface of the specimen. As the sample is polished and inspected under a UV light it is possible to see the pore structure and microcracks.

The sample was first polished down to a level of 0.25 mm. At this level, under the UV light, it is possible to see the pores and cracks which are connected to the surface. The sample was further polished down to 1 mm and 2 mm levels to investigate if the pores and cracks were still connected to the surface. Figure 4 presents the pictures of matrix (PZ) samples subjected to 200°C curing. The pictures of the cross-section were taken under normal light and for the various polishing levels under UV light.

From the investigation under the normal light and 0.25 mm level under the UV light, it was seen that all the samples presented similar pore volumes and pore sizes distribution. The pictures of 1 mm and 2 mm polished levels under the UV light indicated that there was a map cracking associated with 200°C curing (Figure 4).

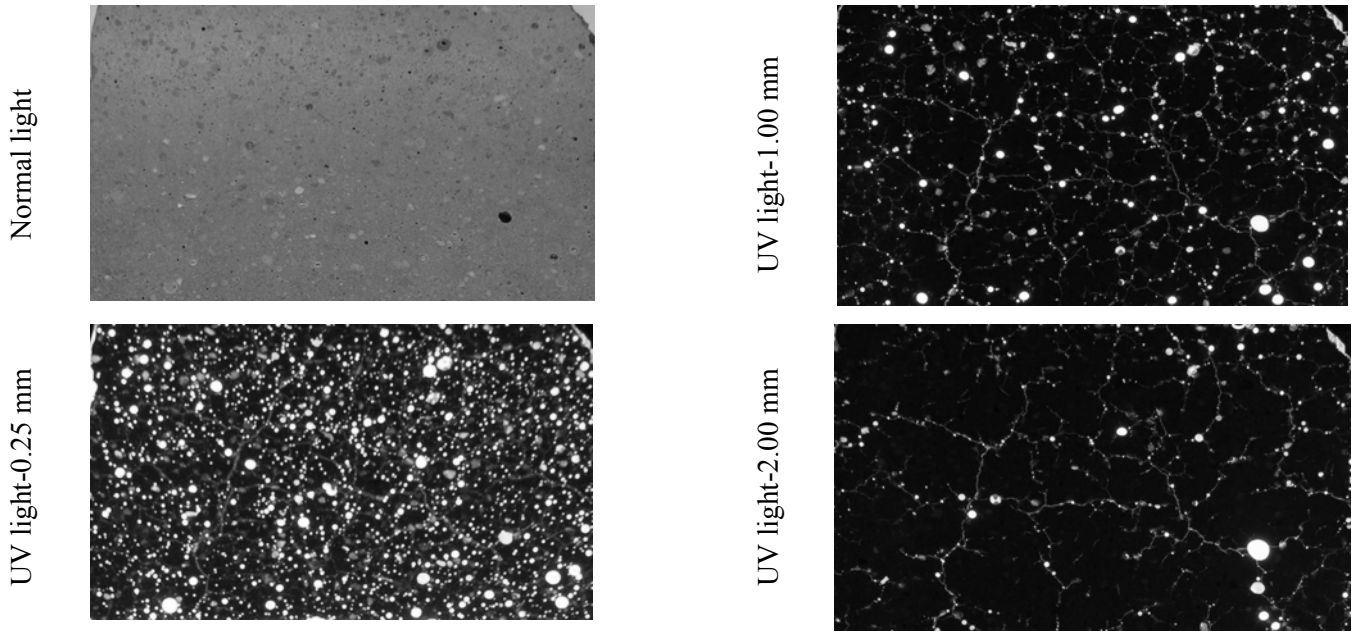

Figure 4. Plane section views of the matrix at 200°C hot curing condition.

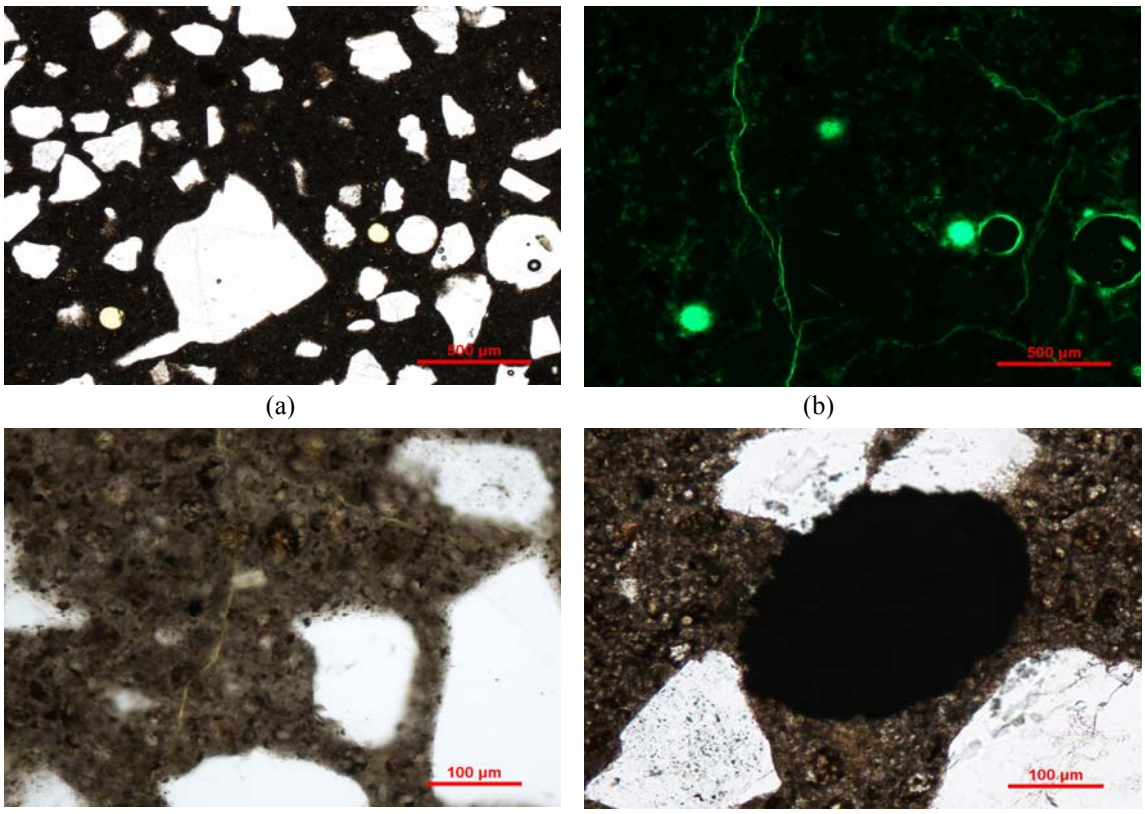

(a) (b)

(c) (d)

Figure 5. View of microcracks in thin section view of the specimen subjected to 200°C (a): plane polarized view at 50x, (b): fluorescence light view at 50x, (c): Microcracks filled with $Ca(OH)_2$, No sign of delayed ettringite formation is observed (plane polarized view at 200x), (d): bond between fiber and cement matrix, the dark circle shows steel fiber (plane polarized view at 200x)

As the sample was polished further down, it was observed that the crack system was connected. 20°C and 65°C steam curing levels did not present any cracks, and the volume of surface connected porosity was low. The pore system of 20°C and 65°C were also not connected with each other. For the thin section analysis, composite samples with a cross-sectional area of approximately 3.5 × 4.5 cm were cut and impregnated with fluorescence epoxy. Then the samples were polished to a thickness of about 30 µm, which allows investigation with a polarising microscope.

With the help of the fluorescence absorbed by the specimen and light filters, it is possible to investigate the crack and pore system. The polarising microscope is also used for mineral identification. Cracks, voids, cement paste and aggregates can be inspected with magnifications of up to 500x.

From Figure 5, the crack system in the samples subjected to 200°C can be observed at 50x magnification. The cracks were further investigated at 200x magnification, crossed polarisation and with a gypsum lamel. With this setting, it was possible to identify calcium hydroxide by its blue-yellow colours. It was observed that the cracks in the sample subjected to 200°C were filled with calcium hydroxide. As seen in thin section of composites cured at 200°C, the interfacial transition zone in the composites with the dense microstructure is characterized by a direct contact between the steel fiber and the matrix (Figure 5d). The CH near the steel fiber reacts with ultrafine silica fume, forming dense C-S-H which fills in the spaces at the interfacial zone, producing increased bond between the matrix and steel fiber. The increased bond allows the efficient transfer of stress between the matrix and steel fibers. Evidence of possible thermally-induced damage such as delayed ettringite formation was also checked. No delayed ettringite formation was observed at hot curing conditions during petrographic investigations.

5 RECENT APPLICATIONS IN ISTANBUL

Gully tops and manhole covers produced in Iston which is a company of Istanbul Metropolitan Municipality, can be used in roads and urban environment for rain water drainage. In these structural elements containing classical reinforcing bars, ultra high performance composites with hybrid steel fibers are used as the matrix. The strength of these matrices reaches up to the compressive strength of 350 MPa. The average load carrying capacity of gully tops and manhole covers produced was 460 kN. This means that D400 load carrying ability in EN 124 is valid for these elements. They are available in different sizes and with special designs such as square gully tops and circular manhole covers. Typical examples are shown in Figure 6.

(a) (b)

Figure 6. Examples produced with high performance hybrid steel fiber reinforced composites (a) gully tops, (b) circular manhole cover

6 CONCLUSION

Based on the tests conducted, it can be concluded that short fibers function as a bridge to eliminate the micro-cracks, and as a result, the tensile strength of composite increases, and the fibers pull out after macrocracks are formed. Thus, the short fibers have little effect on the post-peak response of load versus displacement at the midspan of the beam. The long fibers have no significant effect on preventing micro cracking, however, there is a substantial effect of long fibers on the post-peak response part of curve and also on peak load, resulting in high value of fracture energy. The composites with high strength long steel fibers show a behavior of enhanced toughness and ductility when compared to the composites with normal strength steel fibers. Curing regimes enhance the microstructure of the composites, as a result the compressive strength, specific fracture energy, and flexural strength can be greatly improved. On the other hand, the hot curing condition significantly reduced flexural strength of plain composite probably because the higher curing condition caused the micro cracks in the matrix phase. Petrographic examination showed that a connected crack system forms at 200°C curing condition which is filled with calcium hydroxide. The calcium hydroxide near the steel fiber reacts with ultrafine silica fume, forming dense C-S-H which fills in the spaces at the interfacial zone, producing increased bond strength between the matrix and steel fiber. The gully tops and manhole covers produced to be used in the city infrastructures can be considered as selected applications.

ACKNOWLEDGMENTS

This research was carried out in the Faculty of Civil Engineering at Istanbul Technical University (ITU). The authors wish to acknowledge the financial support of TUBITAK (The Scientific & Technical Research Council of Turkey): Project:106G122, 1007-Kamu.

REFERENCES

Alaee, F.J. 2002. Retrofitting of Concrete Structures Using High Performance Fiber Reinforced Cementitious Composites (HPFRCC), *PhD Thesis*, University of Wales, Cardiff, 220 p.

Alexander,M.G. 1993. From nanometers to gigapascals cementing future, A University of Cape Town Publication, Inaugural Lecture, 23 p.

Balaguru, P., Narahai, R., and Patel, M. 1992. Flexural toughness of steel fibre reinforced concrete. *ACI Materials Journal* 89, 541-546.

Bonneau, O., Lachemi, M., Dallaire, E., Dugat, J. and Aitcin, P-C. 1997. Mechanical properties and durability of two industrial reactive powder concretes. *ACI Materials Journal* 94(4), 286-290.

Dugat, J., Roux, N. and Bernier, G. 1996. Mechanical properties of reactive powder concrete, *Materials and Structures* 29, 233-240.

Feylessoufi, A., Villieras, F., Michot, L.J., De Donato, P., Cases, J.M. and Richard, P. 1996. Water environment and nanostructural network in a reactive powder concrete, *Cement and Concrete Composites* 18, 23-29.

Fritz, C. 1991. Tensile testing of SIFCON in Eds. Reinhardt and Naaman, *Proceedings of 1st International Workshop on HPFRCCs, June 23-26, Mainz*, RILEM, pp. 518-528.

Grünewald, S. & Walraven, J.C., 2002. High strength self-compacting fibre-reinforced concrete: behaviour in the fresh and hardened state, Eds. König, G. et al. *in Proceedings of 6th International Symposium on HSC/HPC,* l., Leipzig, pp. 977-989.

Hillerborg, A., Modeer, M., and Peterson, P.E. 1976. Analysis of crack formation and crack growths in concrete by means of fracture mechanics and finite elements, *Cement and Concrete Research* 6, 773-782.

Ilki, A., Yilmaz, E., Demir, C. And Kumbasar, N. 2004. Prefabricated SFRC jackets for seismic retrofit of non-ductile reinforced concrete columns, *in Proceedings of 13th World Conference on Earthquake Engineering, Vancouver*.

Lange-Kornbak, D. & Karihaloo, B.L. 1998. Design of fibre-reinforced DSP mixes for minimum brittleness. *Adv. Cement Based Materials* 7, 89-101.

Masazza, F. & Costa, U. 1986. Bond: paste-aggregate, paste-reinforcement, and paste-fibers, *in Proceedings of 8th International Congress on the Chemistry of Cement, Rio de Janeiro, Brasil,* pp. 158-180.

Matte, V. & Moranville, M. 1999. Durability of reactive powder composites: Influence of silica fume on the leaching properties of very low water/binder pastes. *Cement and Concrete Composites* 21, 1-9.

Richard, P. & Cheyrezy, M. 1995. Composition of reactive powder concrete, *Cement and Concrete Research* 25, 1501-1511.

Tasdemir, C., Tasdemir, M.A., Mills, N., Barr, B.I.G. and Lydon, F.D. 1999. Combined effects of silica fume, aggregate type, and size on post peak response of concrete in bending, *ACI Materials Journal* 96, 74-83.

Tasdemir, M.A., Tasdemir, C., Akyuz, S., Jefferson, A.D., Lydon, F.D. and Barr, B.I.G. 1998. Evaluation of strains at peak stresses in concrete: A three phase composite model approach, *Cement and Concrete Composites* 20, 301-318.

Vandewalle, L. 1996. Influence of the yield strength of steel fibers on the toughness of fibre reinforced high strength concrete, *in Proceedings of CCMS Symposium, worldwide advances in Structural Concrete and Masonry, Chicago*, pp. 496-495.

Walraven, J. 1999. The evolution of concrete, *Structural concrete, Journal of fib* 1(1), 3-11.